Journal of Alloys and Compounds 509 (2011) L153–L156

Contents lists available at ScienceDirect

Journal of Alloys and Compounds

journal homepage: www.elsevier.com/locate/jallcom

Letter

Sequential interfacial intermetallic compound formation of Cu_6Sn_5 and Ni_3Sn_4 between Sn–Ag–Cu solder and ENEPIG substrate during a reflow process

Jeong-Won Yoon [a,*], Bo-In Noh [a], Jae-Hyun Yoon [a], Han-Byul Kang [b], Seung-Boo Jung [a]

[a] School of Advanced Materials Science and Engineering, Sungkyunkwan University, 300 Cheoncheon-dong, Jangan-gu, Suwon, Gyeonggi-do 440-746, Republic of Korea

[b] High Voltage Electron Microscopy Station, National Institute for Materials Science, 3-13 Sakura, Tsukuba 305-0003, Japan

ARTICLE INFO

Article history:
Received 14 October 2010
Received in revised form
30 December 2010
Accepted 3 January 2011
Available online 5 January 2011

Keywords:
Sn–Ag–Cu solder
Soldering
Intermetallic compounds
Electronic packaging

ABSTRACT

The interfacial reactions between Sn–3.0 wt.% Ag–0.5 wt.% Cu solder and an electroless nickel–electroless palladium–immersion gold (ENEPIG) substrate were investigated. After initial reflowing, discontinuous polygonal-shape $(Cu,Ni)_6Sn_5$ intermetallic compounds (IMCs) formed at the interface. During reflowing for up to 60 min, the interfacial IMCs were sequentially changed in the following order: discontinuous $(Cu,Ni)_6Sn_5$, $(Cu,Ni)_6Sn_5$ and $(Ni,Cu)_3Sn_4$, and embedded $(Cu,Ni)_6Sn_5$ in $(Ni,Cu)_3Sn_4$. The interfacial product variation resulted from the preferential consumption of Cu atoms within the solder and continuous Ni diffusion from the Ni(P) layer.

© 2011 Elsevier B.V. All rights reserved.

1. Introduction

Pb-free solder technology continues to evolve with a combination of innovative solder alloys, flux chemistries, and surface finish technologies offering improved solder joint performance [1,2]. Of the many Pb-free solder alloys, Sn–Ag–Cu solder is the leading candidate to replace Pb-containing solders because of its good comprehensive properties [1,3–6]. Surface finishes also have to be Pb-free and, more importantly, should be able to produce a reliable solder joint when assembled at a high temperature with a Pb-free solder. Presently, there are a series of alternate surface finishes in use throughout the printed circuit board (PCB) industry, such as organic solderability preservatives (OSP), immersion Ag, immersion Sn, direct immersion gold (DIG), electroless nickel–immersion gold (ENIG), and electroless nickel–electroless palladium–immersion gold (ENEPIG). Most of these surface finishes have well-documented records of solder joint reliability over time as they have been used for many years with eutectic Sn–Pb solder. The key question now is whether the solder joints of these surface finishes will be reliable if they are assembled at higher temperatures using Pb-free solders [7].

Of the many surface finishes, ENEPIG is the finish with the widest latitude for a variety of applications [7–11]. ENEPIG was originally introduced in the mid-1990s and did not capture a significant share of the market as expected. Recent mechanical test data indicate an incompatibility with eutectic Sn–Pb solder (specifically, the incompatibility of the Pb with the Pd interferes with the formation of a uniform Ni–Sn intermetallic compound (IMC)) [7]. However, the RoHS (Restriction of Hazardous Substances) Pb-free requirements have made it necessary once again to revisit all available surface finishes, and ENEPIG has again come under close scrutiny as the industry evaluated its capabilities using Pb-free assembly conditions [8]. In the ENEPIG system, the Au layer provides oxidation resistance and better wettability between the solder and the pad. The Pd layer improves the wettability and acts as a diffusion barrier as well. The Ni layer is widely adopted as a diffusion barrier material to prevent the rapid reaction between the Cu and solder induced by Cu diffusion [9]. Peng et al. reported that both the Au and Pd were quickly exhausted within 5 s and then the underlying Ni(P) layer came in contact with the molten solder, forming the $(Cu,Ni)_6Sn_5$ IMC and Ni_3P layer at the Sn–3.0Ag–0.5Cu/Au/Pd/Ni(P) interface [10].

Nevertheless, much remains to be elucidated about the interfacial reactions between Pb-free solder and the ENEPIG substrate. Therefore, in this study, we investigated the interfacial reactions between Sn–3.0Ag–0.5Cu solder and an ENEPIG substrate during a reflow reaction. The formation and growth of sequential interfacial IMCs were studied.

* Corresponding author. Tel.: +82 31 299 4337; fax: +82 31 299 4339.
E-mail address: jwy4918@skku.edu (J.-W. Yoon).

0925-8388/$ – see front matter © 2011 Elsevier B.V. All rights reserved.
doi:10.1016/j.jallcom.2011.01.015

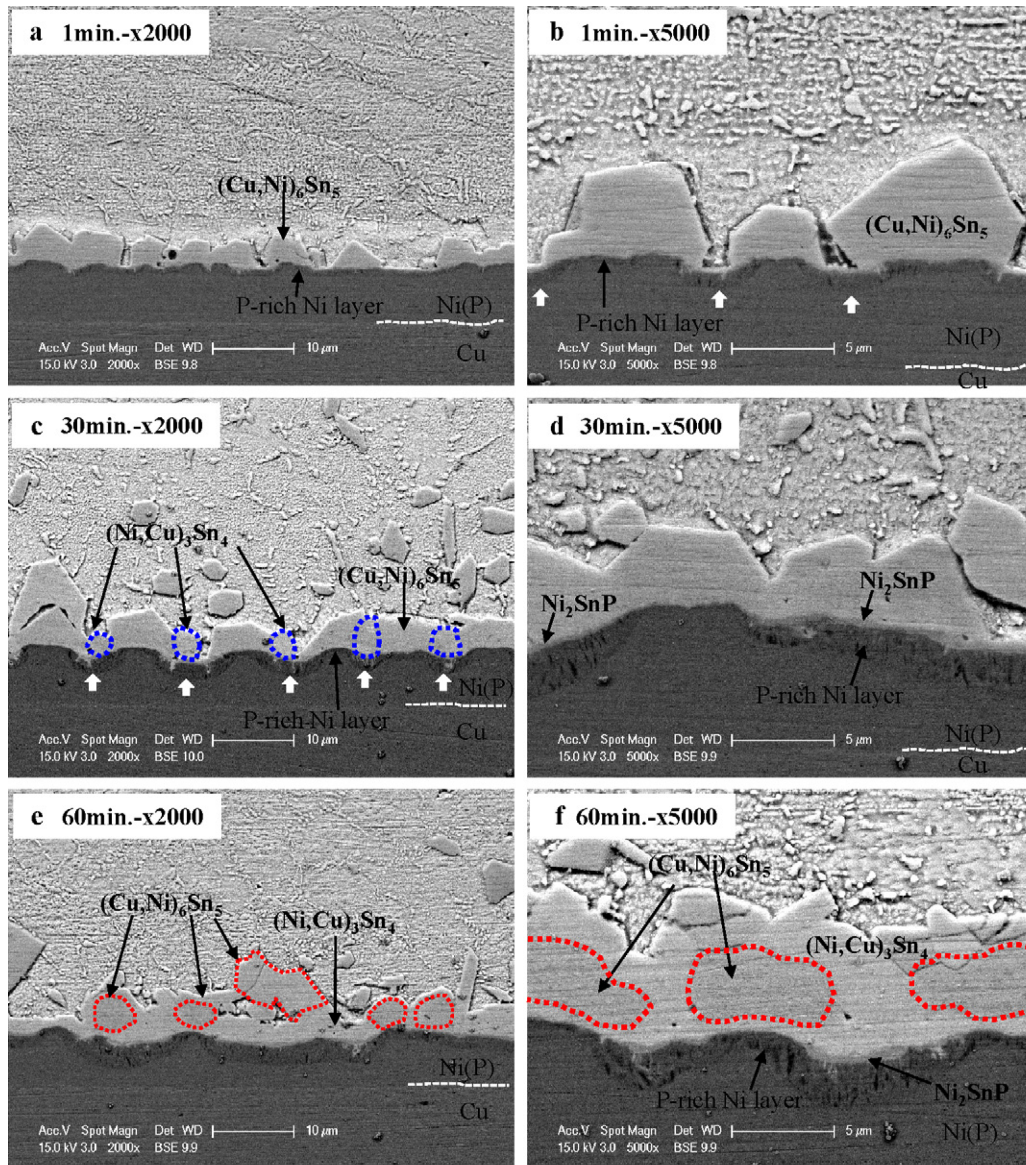

Fig. 1. Cross-sectional SEM images of the Sn–3.0Ag–0.5Cu/ENEPIG interfaces reflowed at 260 °C for various times.

2. Experimental procedures

Ball-grid-array (BGA) solder balls used in this study were made of eutectic Sn–3.0Ag–0.5Cu (in wt.%) with diameters of 450 μm. The test substrate was a flame-retardant-4 PCB. Also, pad opening diameter of BGA substrate was 400 μm. The surface finish of the Cu pads was ENEPIG. The thicknesses of the Ni(P), Pd, and Au layers were approximately 5, 0.1, and 0.08 μm, respectively. The electroless Ni(P) layer contained about 15 at.% P. The electroless Ni(P) plating deposits a mixture of Ni and P because of the use of hypophosphite in the chemical reaction in order to reduce Ni ions. The solder balls were bonded to the BGA substrates in a reflow process employing rosin mildly activated (RMA) flux in a reflow machine (SAT-5100 (reflow mode), Rhesca Co. Ltd., Japan) with a peak temperature of 260 °C for 1–60 min. The time indicates the duration time at the peak temperature of the reflow process. After the reflow process, the samples were cooled to room temperature and cleaned with isopropyl alcohol. After the reflowing and cleaning treatments, the samples were prepared for observation of the interface cross-sections. Common metallographic practices, grinding and polishing, were used to prepare the samples. An etchant consisting of 95% C_2H_5OH–4% HNO_3–1% HCl was used to reveal the cross-sectional microstructure. The microstructures and chemical compositions were observed with a scanning electron microscope (SEM, Philips XL 40 FEG, The Netherlands) equipped with an energy dispersive X-ray spectroscope (EDX). In addition, electron probe micro analyzer (EPMA, JSA8500F, JEOL, Japan) mapping and spot analyses were performed to determine the formation and distribution of the phases formed at the interfaces.

3. Results and discussion

Fig. 1 shows the cross-sectional SEM images of the Sn–Ag–Cu/ENEPIG interfaces reflowed at 260 °C for different reflowing times. Back-scattered electron SEM images were used to provide more distinguishable boundaries of the interfacial layers. During the initial reflowing (1 min), discontinuous polygonal-shape $(Cu,Ni)_6Sn_5$ IMCs formed at the interface, as shown in Fig. 1(a). The topmost Au and Pd layers dissolved into the molten solder, leaving the electroless Ni(P) layer exposed to the molten solder. The reaction between molten Sn–Ag–Cu solder and the electroless Ni(P) layer resulted in the formation of a $(Cu,Ni)_6Sn_5$ layer at the interface. The IMC phase that formed at the interface of the sample reflowed for 1 min was confirmed to be $(Cu,Ni)_6Sn_5$ by EPMA analysis. In addition, the $(Cu,Ni)_6Sn_5$ IMC contained a small amount of Pd. The composition of the IMC was 31.66 at.% Cu, 23.85 at.% Ni, 44.26 at.% Sn, and 0.23 at.% Pd. The Cu in the $(Cu,Ni)_6Sn_5$ IMC layer came from the solder because there was no Cu source except for the solder. In recent years, the interfacial reaction between Sn–Ag–Cu solder and Ni substrates has been intensively studied because of the promising future of Sn–Ag–Cu

as a candidate for Pb-free solders [12–16]. It has been found that the IMCs formed at the Sn–Ag–Cu/Ni interface are very sensitive to the amount of Cu addition in the molten solder. With only 0.5 wt.% addition of Cu to Sn, the interfacial reaction products between the molten solder and the Ni substrate changes from the original $(Ni,Cu)_3Sn_4$ phase to the $(Cu,Ni)_6Sn_5$ phase [12]. Also, a P-rich Ni layer formed at the interface between the $(Cu,Ni)_6Sn_5$ IMC and Ni(P) layer. This P-rich Ni layer consisted of various Ni–P phases, such as Ni_2P, $Ni_{12}P_5$, and Ni_3P, according to our previous TEM study [17]. Due to the consumption of Ni by the formation of the interfacial $(Cu,Ni)_6Sn_5$ IMC, P remained at the top of the remaining Ni(P) layer, resulting in the formation of the P-rich Ni layer consisting of stoichiometric Ni–P phases. In addition, the interface between the $(Cu,Ni)_6Sn_5$ and P-rich Ni layer or P-rich Ni and Ni(P) layer formed an irregular wavy shape, implying more Ni consumption from the electroless Ni(P) layer occurred in certain locations. Indeed, the interfacial morphology underneath the $(Cu,Ni)_6Sn_5$ IMC was convex in shape, but a concave shape interface formed between the discontinuous $(Cu,Ni)_6Sn_5$ IMCs (white arrows in Fig. 1(b)). $(Cu,Ni)_6Sn_5$ IMCs formed first on certain locations of the interface, where the Cu content in the molten solder near the interface was relatively higher than at other locations. Accordingly, the interface between the discontinuous $(Cu,Ni)_6Sn_5$ IMCs continuously was in contact with the molten solder and in that location the Ni atoms of the Ni(P) layer also dissolved into the molten solder, resulting in the formation of the concave shape interface indicated by white arrows in Fig. 1(b). From the results of these interfacial reactions, the original flat Ni(P) interface was converted into a convex–concave shape.

After reflowing for 30 min, $(Ni,Cu)_3Sn_4$ IMCs formed between the discontinuous $(Cu,Ni)_6Sn_5$ IMCs, as shown in Fig. 1(c). The newly formed $(Ni,Cu)_3Sn_4$ IMCs are indicated by blue-dashed lines in Fig. 1(c). A careful comparison of the SEM images shown in Fig. 1(b) and (c) leads us to conclude that the $(Ni,Cu)_3Sn_4$ IMCs formed at the concave sites indicated by white arrows. The formation of the $(Ni,Cu)_3Sn_4$ IMC was caused by a decrease in Cu diffusion into the interface. In other words, the $(Cu,Ni)_6Sn_5$ IMCs, which formed in the previous stage, grew by drawing on the available Cu in the solder. However, the source of Cu in the solder is not infinite. Therefore, during the discontinuous $(Cu,Ni)_6Sn_5$ IMC growth at the interface, the concentration of Cu in the solder will gradually decrease. As a result, the Ni-rich $(Ni,Cu)_3Sn_4$ IMC formed at the concave sites between the $(Cu,Ni)_6Sn_5$ IMCs. In addition, a Ni_2SnP ternary compound was locally observed on the concave sites of the P-rich Ni layer, as shown in Fig. 1(c) and (d). The original Ni(P) layer decreased in thickness, the P-rich Ni layer increased in thickness, and the embossed (convex–concave shape) interface became increasingly noticeable as the reflow time increased. Another interesting reaction was the formation of Kirkendall voids in the crystallized P-rich Ni layer, as shown in Fig. 1(c) and (d). The mechanism of the formation and growth of the Kirkendall voids during reflowing is as follows: Ni atoms diffuse from the original Ni(P) layer to the upper interfacial reaction layer, resulting in a counter diffusion of vacancies; these vacancies accumulate and form a void with prolonged reflow times, which increases the void size.

Table 1
WDX spot analysis results of the interfacial IMCs A and B indicated in Fig. 2(a).

	Point A	Point B
Cu	31.65	10.08
Sn	44.15	56.04
Ni	23.99	33.55
Pd	0.21	0.33
Phase	$(Cu,Ni)_6Sn_5$ + Pd	$(Ni,Cu)_3Sn_4$ + Pd

EPMA mapping analysis was performed to investigate the formation and distribution of the $(Cu,Ni)_6Sn_5$ and $(Ni,Cu)_3Sn_4$ IMCs at the interface. Fig. 2 and Table 1 show the EPMA element mapping and spot analysis results of the Sn–Ag–Cu/ENEPIG interface reflowed for 30 min, respectively. Only two mapping images with regard to elements Cu and Ni are presented here to give an easy comparison between the $(Cu,Ni)_6Sn_5$ and $(Ni,Cu)_3Sn_4$ IMCs. These EPMA analysis results clearly show the coexistence of $(Cu,Ni)_6Sn_5$ and $(Ni,Cu)_3Sn_4$ IMCs. Cu contents of the $(Cu,Ni)_6Sn_5$ and $(Ni,Cu)_3Sn_4$ IMCs were 31.65 and 10.08 at.%, respectively. In addition, the $(Cu,Ni)_6Sn_5$ and $(Ni,Cu)_3Sn_4$ IMCs contained small amounts of Pd (Table 1).

After reflowing for 60 min, the $(Ni,Cu)_3Sn_4$ IMC grew extensively by the reaction of the molten solder and Ni(P) layer. In addition, the $(Cu,Ni)_6Sn_5$ IMCs were sequentially transformed into $(Ni,Cu)_3Sn_4$ IMCs during prolonged reflow times, due to the limited Cu supply from the solder and continuous Ni diffusion from the Ni(P) layer. In other words, the growth of the $(Ni,Cu)_3Sn_4$ IMC consumed the $(Cu,Ni)_6Sn_5$ IMC during prolonged reflow reactions. Consequently, the remaining $(Cu,Ni)_6Sn_5$ IMCs were embedded with $(Ni,Cu)_3Sn_4$ IMCs. The $(Cu,Ni)_6Sn_5$ IMCs are indicated by red-dashed lines in Fig. 1(e) and (f). During reflowing between 30 and 60 min, the growth of the $(Cu,Ni)_6Sn_5$ IMC had already been completed and the $(Ni,Cu)_3Sn_4$ IMC was a predominant interfacial product. Compared to the compositions for these two IMC layers, the Cu content of the $(Ni,Cu)_3Sn_4$ IMC was much lower than that of the $(Cu,Ni)_6Sn_5$ IMC

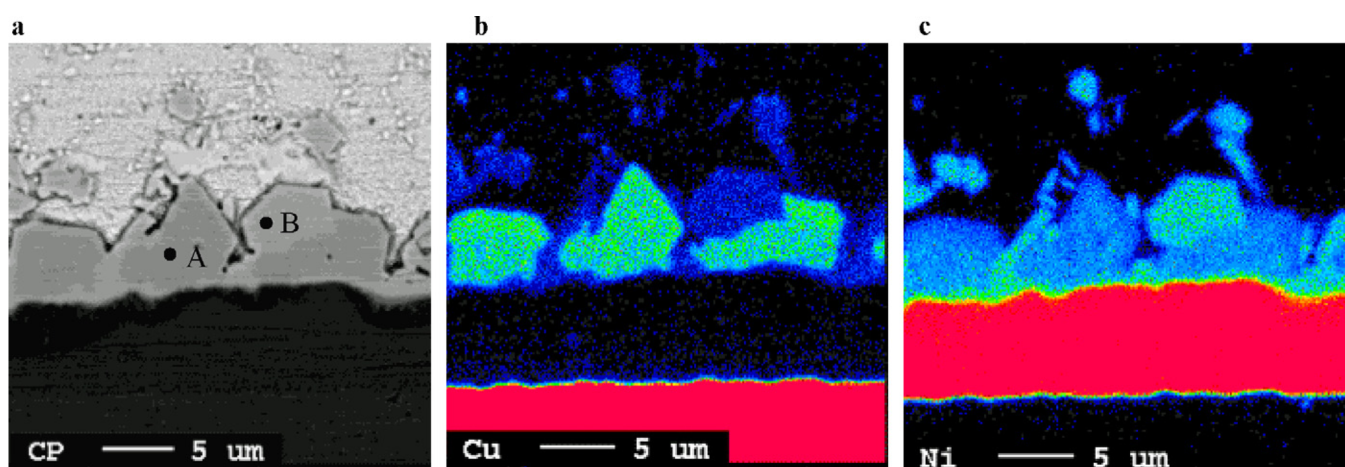

Fig. 2. EPMA mapping analysis results of the Sn–3.0Ag–0.5Cu/ENEPIG interface reflowed at 260 °C for 30 min. Only two mapping images with regard to elements Cu and Ni are presented here to give an easy comparison between $(Cu,Ni)_6Sn_5$ and $(Ni,Cu)_3Sn_4$ IMCs.

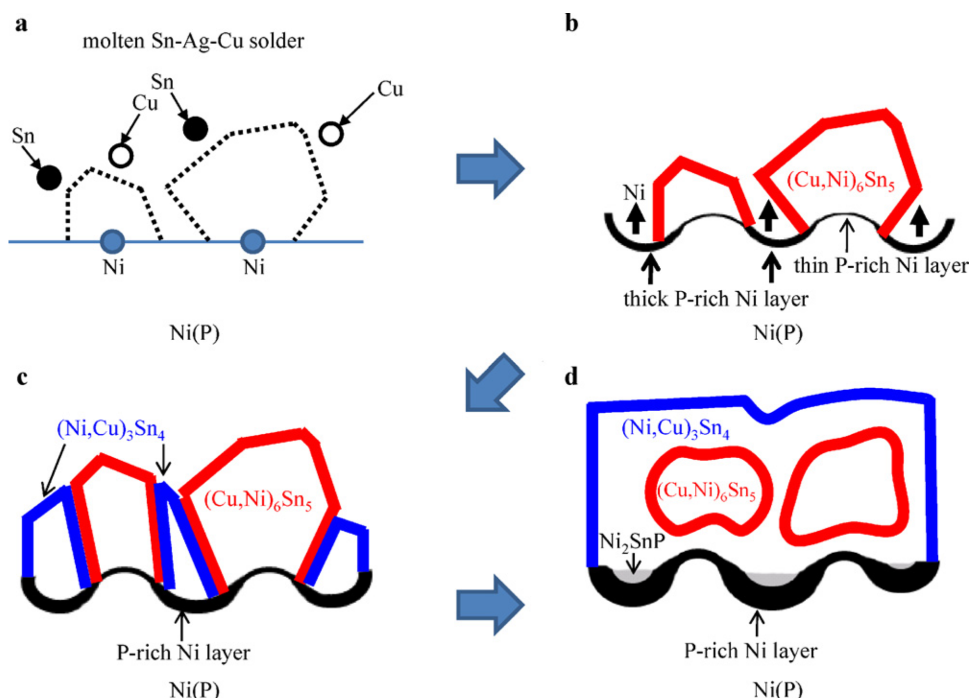

Fig. 3. Schematic diagram of the sequential interfacial reactions of the Sn–3.0Ag–0.5Cu/ENEPIG joints reflowed at 260 °C for various times.

(see Table 1). Therefore, the growth of the $(Ni,Cu)_3Sn_4$ IMC layer on the Ni(P) substrate would have been relatively easy due to the finite Cu content in the molten solder. As a result, the growth of the $(Ni,Cu)_3Sn_4$ IMC consumed the existing $(Cu,Ni)_6Sn_5$ IMC. Fig. 3 presents a schematic diagram of the sequential interfacial reactions between the Sn–3.0Ag–0.5Cu solder and ENEPIG substrate during reflowing at 260 °C, based on Figs. 1 and 2. This schematic diagram clearly illustrates the sequence of the interfacial reactions between the Sn–Ag–Cu solder and ENEPIG substrate with the reflow treatment. In the initial reflow process, discontinuous $(Cu,Ni)_6Sn_5$ IMCs formed at the interface and the P-rich Ni layer formed at the interface between the $(Cu,Ni)_6Sn_5$ and Ni(P) layer (Fig. 3(a) and (b)). As the reflow time increased, the $(Ni,Cu)_3Sn_4$ IMCs formed between the discontinuous $(Cu,Ni)_6Sn_5$ IMCs (Fig. 3(c)). With prolonged reflow times, the $(Ni,Cu)_3Sn_4$ IMC grew extensively and the remaining $(Cu,Ni)_6Sn_5$ IMCs were embedded with $(Ni,Cu)_3Sn_4$ IMCs (Fig. 3(d)).

4. Conclusions

In this study, we investigated the interfacial reactions between the Sn–3.0Ag–0.5Cu solder and ENEPIG substrate during a reflow reaction. In the early stage of reflow, discontinuous polygonal-shape $(Cu,Ni)_6Sn_5$ IMCs formed at the interface. The formation of $(Cu,Ni)_6Sn_5$ grains is due to the locally higher Cu content in the liquid solder near the interface. In addition, a P-rich Ni layer formed at the interface between the $(Cu,Ni)_6Sn_5$ and Ni(P) layer. The locations where interfaces between the discontinuous $(Cu,Ni)_6Sn_5$ IMCs were continuously in contact with the molten solder allowed for Ni atoms of the Ni(P) layer to further dissolve into the molten solder, resulting in the formation of a concave shape interface. As the reflow time increased, the $(Ni,Cu)_3Sn_4$ IMCs formed at the concave sites between the discontinuous $(Cu,Ni)_6Sn_5$ IMCs. In addition, a Ni_2SnP ternary compound was locally observed on the concave sites of the P-rich Ni layer. With prolonged reflow times, the $(Ni,Cu)_3Sn_4$ IMC grew extensively and the $(Cu,Ni)_6Sn_5$ IMCs were sequentially transformed into $(Ni,Cu)_3Sn_4$ IMCs. Consequently, the remaining $(Cu,Ni)_6Sn_5$ IMCs were embedded with $(Ni,Cu)_3Sn_4$ IMCs. The original Ni(P) layer was reduced and the P-rich Ni layer became larger as the reflow time increased. We considered that the interfacial product variation resulted from the preferential consumption of Cu atoms within the solder and continuous Ni diffusion from the Ni(P) layer.

Acknowledgements

This work was supported by the WCU program of the Korea Science & Engineering Foundation funded by the Korean Government (MOEHRD) (Grant No. R32-2008-000-10124-0).

References

[1] M. Abtew, G. Selvaduray, Mater. Sci. Eng. R 27 (2000) 95–141.
[2] C.M.L. Wu, D.Q. Yu, C.M.T. Law, L. Wang, Mater. Sci. Eng. R 44 (2004) 1–44.
[3] Y. Gao, C. Zou, B. Yang, Q. Zhai, J. Liu, E. Zhuravlev, C. Schick, J. Alloys Compd. 484 (2009) 777–781.
[4] Y.T. Chen, Y.T. Chan, C.C. Chen, J. Alloys Compd. 507 (2010) 419–424.
[5] F.X. Che, W.H. Zhu, E.S.W. Poh, X.W. Zhang, X.R. Zhang, J. Alloys Compd. 507 (2010) 215–224.
[6] A.K. Gain, T. Fouzder, Y.C. Chan, A. Sharif, N.B. Wong, W.K.C. Yung, J. Alloys Compd. 506 (2010) 216–223.
[7] G. Milad, D. Gudeczauskas, Met. Finish. 104 (2006) 33–36.
[8] G. Milad, M. Orduz, Met. Finish. 105 (2007) 25–28.
[9] Y.W. Yen, P.H. Tsai, Y.K. Fang, S.C. Lo, Y.P. Hsieh, C. Lee, J. Alloys Compd. 503 (2010) 25–30.
[10] S.P. Peng, W.H. Wu, C.E. Ho, Y.M. Huang, J. Alloys Compd. 493 (2010) 431–437.
[11] W.H. Wu, C.S. Lin, S.H. Huang, C.E. Ho, J. Electron. Mater. 39 (2010) 2387–2396.
[12] C.E. Ho, R.Y. Tsai, Y.L. Lin, C.R. Kao, J. Electron. Mater. 31 (2002) 584–590.
[13] W.T. Chen, C.E. Ho, C.R. Kao, J. Mater. Res. 17 (2002) 263–266.
[14] J.W. Yoon, S.B. Jung, J. Alloys Compd. 448 (2008) 177–184.
[15] H.B. Kang, J.H. Bae, J.W. Lee, M.H. Park, Y.C. Lee, J.W. Yoon, S.B. Jung, C.W. Yang, Scr. Mater. 60 (2009) 257–260.
[16] H.B. Kang, J.H. Bae, J.W. Yoon, S.B. Jung, J. Park, C.W. Yang, Scr. Mater. 63 (2010) 1108–1111.
[17] H.B. Kang, J.W. Lee, J.H. Bae, M.H. Park, J.W. Yoon, S.B. Jung, J.S. Ju, C.W. Yang, J. Mater. Res. 23 (2008) 2195–2201.